PHYSICAL REVIEW D **86,** 063520 (2012)

CMB polarization impact on cosmological constraints

Sudeep Das[1,3] and Eric V. Linder[1,2]

[1]*Berkeley Center for Cosmological Physics and Berkeley Lab, University of California, Berkeley, California 94720, USA*
[2]*Institute for the Early Universe WCU, Ewha Womans University, Seoul, Korea*
[3]*High Energy Physics Division, Argonne National Laboratory, 9700 S. Cass Avenue, Argonne, Illinois 60439, USA*
(Received 13 July 2012; published 19 September 2012)

Cosmic microwave background (CMB) polarization encodes information not only on the early universe but also dark energy, neutrino mass, and gravity in the late universe through CMB lensing. Ground-based surveys, such as ACTpol, PolarBear, and SPTpol, significantly complement cosmological constraints from the Planck satellite, strengthening the CMB dark energy figure of merit and neutrino mass constraints by factors of 3–4. This changes the dark energy probe landscape. We evaluate the state of knowledge in 2017 from ongoing experiments including dark energy surveys (supernovae, weak lensing, galaxy clustering), fitting for dynamical dark energy, neutrino mass, and a modified gravitational growth index. Adding a modest strong lensing time delay survey improves those dark energy constraints by a further 32%, and an enhanced low-redshift supernova program improves them by 26%.

DOI: 10.1103/PhysRevD.86.063520 PACS numbers: 98.70.Vc, 95.36.+x, 98.80.Es

I. INTRODUCTION

The cosmic microwave background (CMB) radiation temperature and polarization power spectra have provided a cornucopia of cosmological information on both the early and late universe [1–6]. In the next five years considerably more detailed information will be delivered by the Planck satellite [7] and ground-based, high-resolution polarization experiments, such as ACTpol [8], POLAR [9], PolarBear [10] and SPTpol [11].

Such high-resolution experiments carry substantial information on not only the primordial perturbations, but on the matter density power spectrum at redshifts $z \approx 1$–5 as well. The matter perturbations gravitationally lens the primordial CMB and from the reconstructed deflection field one can extract the cosmological parameters that impact the matter power spectrum. These include properties of dark energy, including the time variation of its equation of state, the sum of neutrino masses, and the gravitational growth index to test general relativity.

In this article we focus on the role of such near-term CMB polarization information in constraining these cosmological parameters simultaneously, since all of them affect the CMB lensing. We will also bring in other dark energy survey information expected within the five year horizon to complement the CMB, to give an overall reasonable assessment of the constraints in 2017. We emphasize that the CMB is the main focus of this article and we take a fiducial combination of dark energy surveys with no intent to study all possible permutations.

Section II gives a brief review of CMB lensing and describes the near-term CMB data sets. In Sec. III we present the cosmological parameter set and the Fisher matrix constraints from the CMB, then add in various dark energy probes. Leverage from possible further near-term data is discussed in Sec. IV.

II. POLARIZATION AND LENSING

Recent high-resolution instruments have enabled us for the first time to robustly detect and utilize minute distortions in the CMB due to its interactions with the inhomogeneities in the dark matter distribution in the universe, and with the hot gas in galaxy clusters. One unique upshot has been the recent CMB-only detection and characterization of the gravitational lensing signal, marking the beginnings of an exciting new field [12,13]. The CMB lensing effect is conceptually simple: CMB photons propagating through the universe get deflected by inhomogeneities in the large scale distribution of matter, so that the image of the CMB at our end is a distorted version of the image at the last scattering surface where the CMB was formed [14]. The rms deflection of the CMB photon is about 3 arcminutes on the sky and is caused by all the structure between us and the last scattering surface, with the main contribution coming from the redshift range $z \approx 1$–5. The deflections are coherent over degree angular scales, and coherently distort arcminute-scale anisotropies in the CMB. This leads to a smearing of the peaks in the CMB temperature power spectrum and also the generation of small-scale B-mode polarization from the lensing of E-modes. A unique aspect of lensing is that it induces a specific form of non-Gaussianity in the CMB, which can then be used to reconstruct the projected dark matter potential field. This projected lensing potential depends on both the geometry and the growth of structure. Dark energy affects both geometry and growth, and massive neutrinos affect the growth of structure by suppressing the amplitude of matter fluctuations on scales smaller than their free streaming length. These effects make CMB lensing one of the most promising probes of neutrino mass sum and dark energy behavior [15,16].

The next generation of polarization-enabled high-resolution CMB experiments will be primarily CMB

lensing machines. Since both temperature and polarization are lensed by the same large scale deflection field, the inclusion of polarization improves the fidelity of the lensing reconstruction. Also, foregrounds are expected to be much lower in polarization, enabling us to use more modes to perform CMB lensing reconstruction than temperature alone. (Although in this article we use a conservative limit of $\ell_{\rm max} = 3000$ for both temperature and polarization modes, the expectation is that we should be able to use modes up to ~5000 in polarization.) For the projections made here, we consider an amalgam of high-resolution CMB polarization data from ACTpol, PolarBear, and SPTpol. We assume a total of 10,000 deg^2 covered at the depth of 5 μK-arcmin in temperature and 7 μK-arcmin in polarization. Although the resolutions of these experiments vary, we assume a uniform FWHM of 1 arcmin for the entire combined dataset. This is justified because, at the depth considered here, and with the range of CMB multipoles used for the lensing reconstruction, the projections are largely insensitive to the beam width as long as it is below 4 arcmin.

For the CMB-only projections (especially those not including lensing information) large degeneracies exist in several beyond-ΛCDM parameters. For the projections in such cases (e.g., w_0-w_a contour for Planck without lensing), the large Fisher error ellipses shown here should be viewed as qualitative.

III. COSMOLOGICAL CONSTRAINTS

A. CMB surveys

The usual set of cosmological parameters describing the vanilla model is the dimensionless physical baryon density $\omega_b = \Omega_b h^2$, cold dark matter density $\omega_c = \Omega_c h^2$, dark energy density $\Omega_{\rm de}$, spectral index of scalar perturbations n_s, optical depth τ, and amplitude of mass perturbations σ_8. The dimensionless Hubble parameter h is defined implicitly through the summation of the energy densities to the critical value: we restrict our analysis to a spatially flat universe as a theoretical prior.

We enlarge this set of parameters by considering the main physical quantities that would impact the matter power spectrum and hence CMB lensing. Dark energy other than a cosmological constant is likely to have a dynamical equation of state $w(a)$, with a being the cosmic scale factor. The form $w(a) = w_0 + w_a(1 - a)$ was fit from exact solutions of scalar field theories [17] and derived as a calibration relation for observables accurate at the 0.1% level [18], so we include the two parameters w_0, the present dark energy equation of state, and w_a, a measure of its time variation.

Neutrinos have mass, and this affects the matter power spectrum, so we include the dimensionless neutrino energy density $\omega_\nu = \Omega_\nu h^2$ as a parameter. Note that the sum of the neutrino masses $\sum m_\nu = 94\omega_\nu$ eV. Finally, although within general relativity the background densities determine the growth rate of matter density perturbations, in other theories the strength of gravity, the effective Newton's constant, has an additional impact. To test for deviations from general relativity (GR) we include the gravitational growth index γ [19], a single parameter shown to describe the growth deviations in several models of scale-independent modified gravity at the 0.1% level [20]. These ten parameters are simultaneously fit; as we will see, accounting for only a subset of the additional parameters can significantly overestimate the constraining power, or bias the results in the case of an improper fiducial (e.g., assuming zero neutrino mass). Fiducial values are given in Table I.

Figure 1 illustrates the constraints in the dark energy equation of state plane for various cases using CMB data. The most important lesson is that including CMB lensing information gives dramatic improvement in the constraints. The second lesson is that, as just stated, fixing parameters such as neutrino mass, rather than simultaneously fitting for them, can underestimate the errors. Finally, we see that near-term, high-resolution ground-based CMB polarization surveys generate significantly tighter constraints. This gain applies to all parameters, not just the dark energy equation of state ones, as Table I shows. In particular, the gain in the constraint on neutrino mass (assuming GR, here only, to break the $\gamma - \sigma_8$ degeneracy) is significant, as shown in Fig. 2.

B. Dark energy surveys

We now consider the addition of dark energy survey probes, treating as fiducial CMB data the combination of Planck plus 10,000 deg^{2}of ground-based, high-resolution data, accounting for CMB lensing and fitting all parameters simultaneously. These other probes may bring in further,

TABLE I. 1σ constraints from forthcoming CMB data on cosmological parameters, from the Planck satellite and from Planck plus 10,000 deg^2 of high-resolution, ground-based CMB polarization data. Gain shows the improvement due to adding the ground data. The degeneracy ("d") between the parameters σ_8 and γ is not well broken. The derived fiducial $h = 0.708$ and $\sum m_\nu = 0.15$ eV.

	ω_b	ω_c	ω_ν	$\Omega_{\rm de}$	n_s	τ	σ_8	w_0	w_a	γ
Fiducial	0.02258	0.1093	0.001596	0.734	0.963	0.086	0.8	−1	0	0.55
σ (Planck)	0.000137	0.00117	0.00175	0.124	0.00337	0.00426	d	1.10	2.48	d
σ(Planck + 10 k	0.0000492	0.000682	0.000666	0.042	0.00207	0.00297	d	0.305	0.642	d
Gain	2.78	1.72	2.63	2.95	1.63	1.43	d	3.61	3.86	d

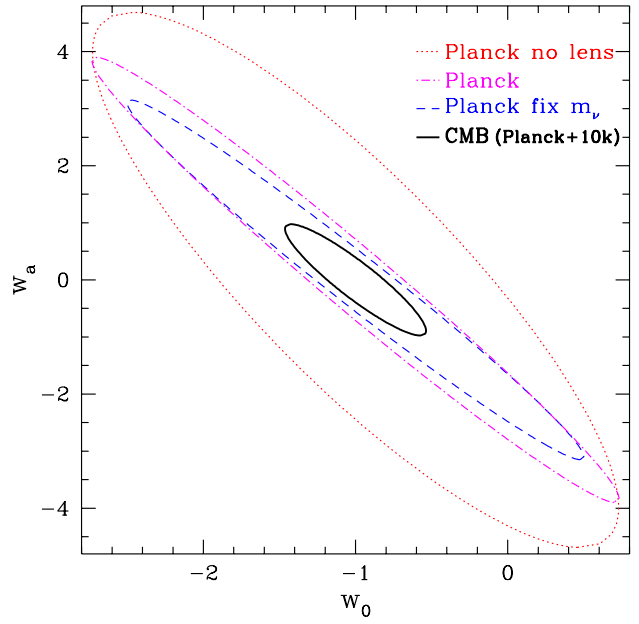

FIG. 1 (color online). 68% confidence contours on the dark energy equation of state parameters w_0 and w_a, marginalized over all remaining parameters, for various cases of CMB data. All data uses both CMB temperature and polarization power spectra, but in the "no lens" case does not use the information in the CMB lensing deflection field. The "fix m_ν" case fixes the sum of neutrino masses to the fiducial. Ground based, high-resolution data is included in the $+10k$ case and delivers a substantial improvement in constraints.

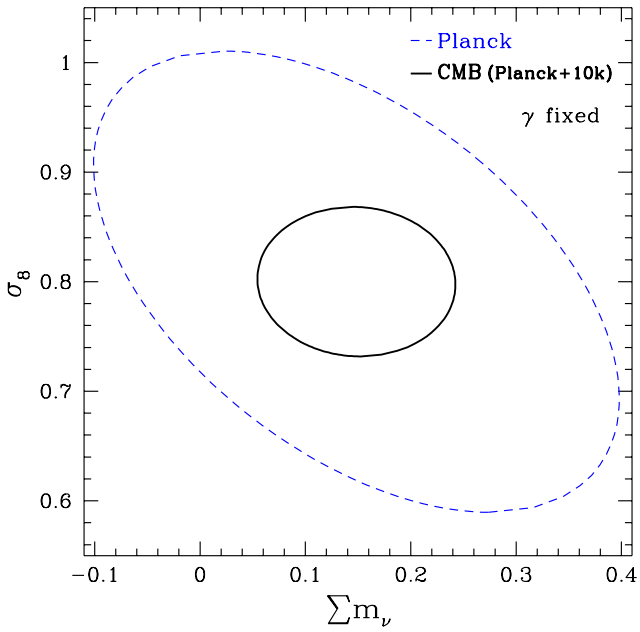

FIG. 2 (color online). 68% confidence contours on the parameters σ_8 and $\sum m_\nu$, marginalized over all remaining parameters, except the growth index γ which is fixed at its GR value, for various cases of CMB data.

nuisance parameters, which we also marginalize over. Our guiding principle is to consider surveys essentially underway, giving a quantitative level of results neither optimistic nor pessimistic, but reasonably expected within five years.

Distances from the Type Ia supernova (SN) magnitude-redshift measurements play an important role in constraining the dark energy equation of state. We adopt a combination of projected data of 150 SN at $z = 0.03$–0.08 from the Nearby Supernova Factory [21], 1000 SN at $z = 0.1$–1 from the Dark Energy Survey (DES [22]) and other SN surveys, and 42 SN at $z = 1$–1.7 from Hubble Space Telescope surveys. These numbers are not to be interpreted as the total numbers expected (for example DES should get several thousand SN) but rather the number in line with the level of systematic errors adopted. Systematic uncertainties of $0.02(1 + z)$ mag per 0.1 redshift bin are added in quadrature with individual intrinsic dispersions of 0.13 mag. In Sec. IV we consider the possibility of enhanced data, but we adopt this as a canonical, reasonable data set.

Weak gravitational lensing (WL) probes both distances and growth and is key in breaking the degeneracy between σ_8 and γ. We model the projected data on DES, with 5000 deg^2 of galaxy shears measured at a density of $n_g = 12/\text{arcmin}^2$ and a median redshift depth $z_{\text{med}} = 0.7$. Systematic uncertainties with priors in photometric redshift bias of 10^{-3}, in photo-z scatter of 10^{-3}, multiplicative shear of 10^{-2}, and additive shear of 10^{-5} are

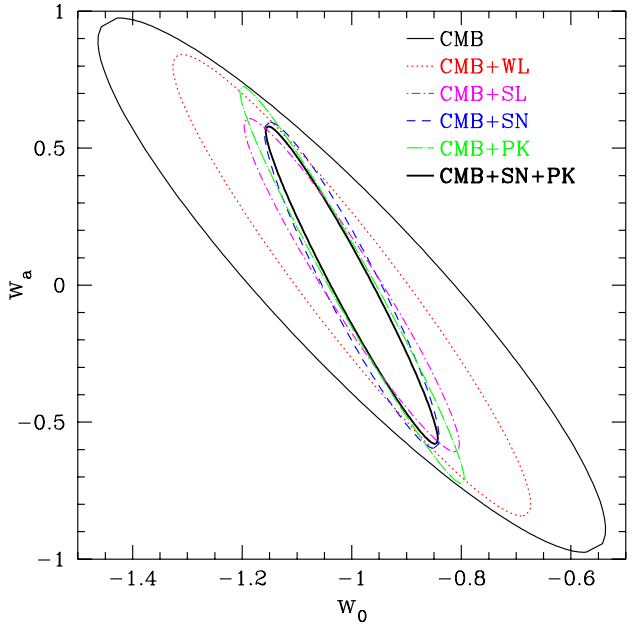

FIG. 3 (color online). 68% confidence contours of w_0 and w_a for combinations of other surveys with CMB data. SN surveys are particularly complementary for dark energy parameters, but galaxy clustering (PK) is constraining in other parameters such as γ. The fiducial combination of SN + PK surveys with CMB data improves the area uncertainty (figure of merit) by a factor of 8.1 over CMB alone.

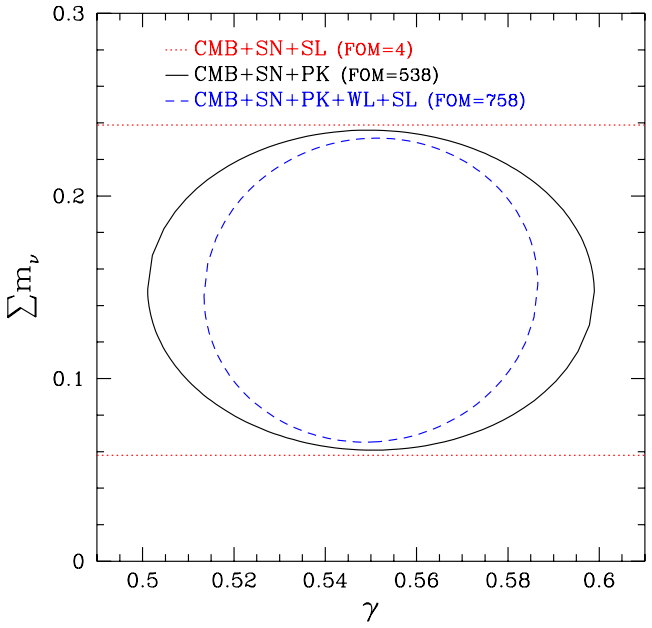

FIG. 4 (color online). 68% confidence contours on the sum of neutrino masses $\sum m_\nu$ and gravitational growth index γ, marginalized over all remaining parameters, for combinations of other surveys with CMB data. PK breaks the growth covariance, determining γ: CMB data provides nearly all of the constraint on neutrino mass, to an uncertainty of 0.058 eV. Inverse contour areas are indicated by the values FOM.

used. See Ref. [23] for more details on the weak lensing computational code that includes the whole set of our cosmological parameters affecting growth.

Galaxy clustering can be used as a distance (and Hubble parameter) estimator through the baryon acoustic oscillation scale of wiggles in the matter power spectrum, and a probe of growth through the full shape and amplitude of the power spectrum. Angular anisotropies due to peculiar motions, called redshift space distortions, carry information on the growth rate and constrain both the background expansion and the gravitational growth index γ. We model the projected power spectrum data (PK) on the ongoing Baryon Oscillation Spectroscopic Survey [24], using the power spectrum out to $k_{\rm max} = 0.125h/{\rm Mpc}$ and allowing for galaxy bias fit parameters in each of the redshift bins at $z = 0.35, 0.6$.

Figure 3 illustrates the impact of complementarity of the dark energy surveys, one by one, with the CMB polarization data. The differing orientation of the confidence contours shows further complementarity will come from combining several probes. Indeed, the combination CMB + SN + PK improves the contour area figure of merit (FOM $= 1/\sqrt{\det {\rm COV}[X, Y]}$, where COV is the covariance matrix of parameters X, Y, marginalized over all others) by 44% over CMB + SN and 42% over CMB + PK.

However, gains are simultaneously made in the other parameters; in particular, PK allows separate and precise determinations of σ_8 and γ. Figure 4 shows the uncertainties in the $\gamma - \sum m_\nu$ plane. Note how the CMB is capable of determining the neutrino masses, but without separate growth information from PK the degeneracy between σ_8 and γ prevents a reasonable determination of γ.

From Fig. 3 we see there is good complementarity between each of PK, SN, and strong lensing time delays (SL, discussed in Sec. IV A). WL is also complementary but has less leverage at the level of systematics taken for DES. If the systematics can be overcome, in DES or a further future experiment, then WL will be more powerful. On the other hand, the complementarity of the other probes indicates that if WL falters, then this will not badly harm our knowledge of the cosmological parameters. In particular, in the presence of PK data SL can meet or exceed the contributions of WL. The one exception is the gravitational growth index γ.

The parameter constraints from our fiducial projections for data within the next five years, representing the combination CMB + SN + PK, appear in Table II. We also present the results including WL and SL as in Sec. IV A.

IV. ADDITIONAL INFORMATION

A. Time delay distances

Geometric measures of distance ratios through strong gravitational lensing time delays (e.g., of quasars lensed by galaxies) have especially good complementarity with SN [25]. While this technique, which requires both imaging and spectroscopy for accurate lens mass modeling, is not a canonical part of any of the surveys we have discussed, individual groups are pursuing time delay surveys [26–28].

Here we take a modest version of the survey proposed in Ref. [25], requiring detailed measurement of a total of 38

TABLE II. 1σ constraints from forthcoming data on cosmological parameters, from various combinations of probes on the 2017 time scale. We consider the first combination, CMB + SN + PK, to be the baseline and also show various extensions. Here FOMw = FOM$[w_0, w_a]$ is the dark energy figure of merit and FOMν = FOM$[\sum m_\nu, \gamma]$ is a growth figure of merit.

	$10^5\omega_b$	$10^4\omega_c$	$10^4\omega_\nu$	$\Omega_{\rm de}$	n_s	σ_8	w_0	w_a	γ	FOMw	FOMν
σ(CMB + SN + PK)	4.76	6.47	6.21	0.00507	0.00200	0.0110	0.103	0.382	0.0322	103	538
σ(CMB + SN + PK + WL)	4.71	5.85	5.97	0.00470	0.00192	0.00934	0.0927	0.339	0.0256	120	704
σ(CMB + SN + PK + SL)	4.74	6.03	6.12	0.00414	0.00195	0.0107	0.0801	0.292	0.0319	135	551
σ(CMB + SN + PK) + WL + SL	4.70	5.63	5.89	0.00403	0.00189	0.00808	0.0774	0.280	0.0241	147	758

time delay systems over the range $z = 0.1$–0.6, each of 5% accuracy in the time delay distance (equivalent to 2% accuracy per 0.1 bin in redshift). To obtain the high resolution needed to accurately map the multiple images and create a robust lens mass model (see, e.g., Ref. [29,30]), Hubble Space Telescope imaging is required. As a rough estimate, each time delay system requires ~6 orbits [31], so the entire program (not counting the systems already investigated) would take ~230 orbits. A restricted range of $z = 0.3$–0.6 only loses 2% on FOM(w_0, w_a) and FOM(m_ν, γ) while reducing the time to ~150 orbits.

The cosmological impact of such a strong lensing (SL) survey is dramatic. The complementarity with SN (and other probes) is evident in Fig. 3. Added to CMB + SN, SL provides a gain of 52% in dark energy equation of state FOM. Even added to the fiducial CMB + SN + PK, the constraints improve further, by 32%, as illustrated in Fig. 5. The gain over the fiducial survey combination is 18% in Ω_m.

While the time delay probe is not as mature at the moment as other techniques, its potential leverage makes it worth more detailed consideration for allocating observing time over the next five years. If systematic uncertainties can be controlled to better than 5% per time delay system, then the observing time required can be reduced. That is, we assumed 2% distance per bin; if systematics can be reduced to 3.5% per system then only half as many systems need to be used. Recent work [32] also offers hope for using simpler two-image systems.

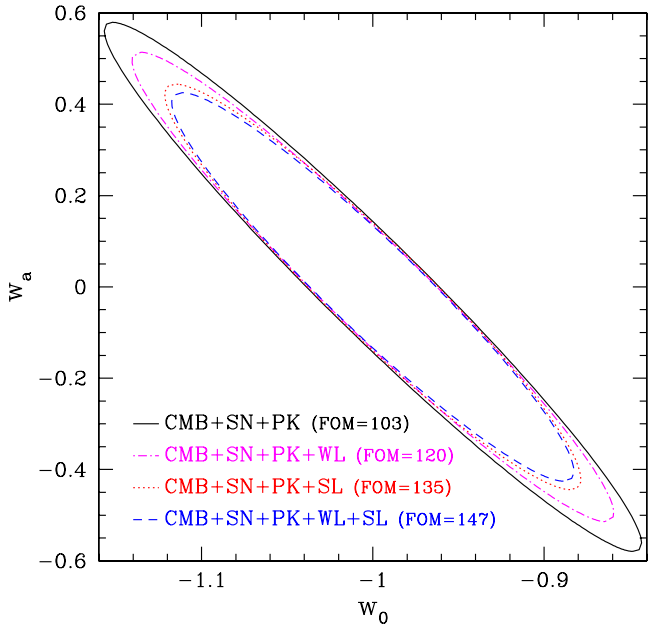

FIG. 5 (color online). 68% confidence contours of w_0 and w_a for combinations of strong lensing time delay data (SL) with other surveys. Even relative to the fiducial CMB + SN + PK, the SL data has further complementarity, improving the FOM by 32%, a stronger gain than from WL.

B. Enhanced surveys

We now consider the impact on cosmological parameter estimation for some specific enhancements to the surveys. This is not an optimization exercise but rather an exploration of possible further leverage.

First we look at the CMB ground polarization data. While observations from the South Pole are restricted to ~4000 deg^2 of sky, mid-latitude sites in both hemispheres could do larger areas. We thus consider how the cosmology constraints vary for areas other than our fiducial 10,000 deg^2 (at the same depth). For areas where Planck and ground-based surveys overlap, we add their inverse noises in quadrature. Figure 6 illustrates the dependence of the dark energy and neutrino-gravity (growth) figures of merit on the area of the ground-based survey.

Another possibility is to increase the area of the spectroscopic galaxy survey beyond the 10 000 deg^2 of our fiducial. Note that a greater area survey would likely extend beyond our five year horizon. Figure 7 shows that the growth figure of merit capturing the sum of neutrino masses $\sum m_\nu$ and the gravity growth index γ continues to increase significantly for larger surveys, while the dark energy figure of merit is closer to saturation.

For the supernova dark energy probe, a particularly useful enhancement on the five year time scale is a larger nearby supernova survey with tightly controlled systematics. Our fiducial involved 150 supernovae with a systematics floor of 0.021 mag. Considerable effort is ongoing at improving supernova systematics with highly calibrated spectrophotometry *à la* the Nearby Supernova

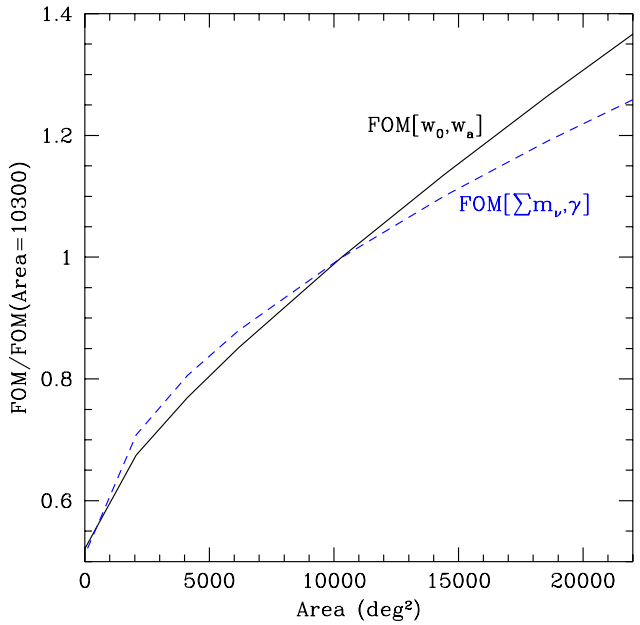

FIG. 6 (color online). For the baseline survey combination CMB + SN + PK the dark energy and growth figures of merit increase as shown with increasing area of the ground-based CMB survey.

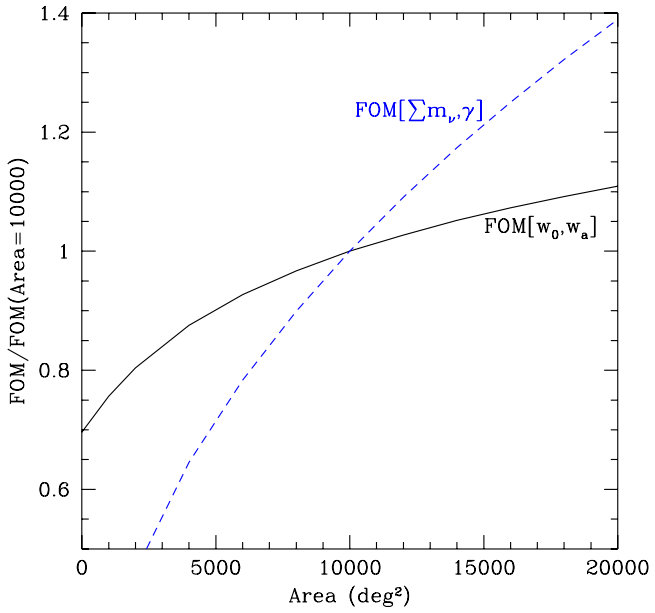

FIG. 7 (color online). For the baseline survey combination CMB + SN + PK the dark energy and growth figures of merit increase with increasing area of the galaxy clustering (PK) survey. The growth figure of merit, describing our knowledge of neutrino mass and ability to test Einstein gravity, improves more quickly with area.

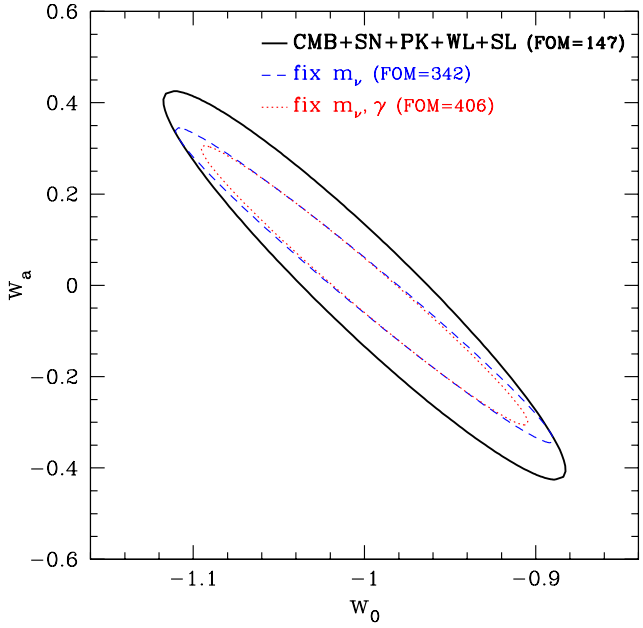

FIG. 8 (color online). 68% confidence contours of w_0 and w_a significantly shrink if we neglect, or assume perfect knowledge of, neutrino mass and gravity. Such assumptions are not generally justified.

Factory [21] and near infrared observations *à la* the Carnegie Supernova Project [33], both offering promising leads. We therefore consider an enhanced program with 300 supernovae in $z = 0.03$–0.08 with a systematics floor over this range of 0.008 mag. This seems within the realm of practicality for our five year time scale.

Such a supernova program yields significant improvements. For the combination CMB + SN + PK the w_0-w_a FOM rises by 26%, from 103 to 129.

C. Fixing parameters

Our approach has been to include all the main cosmological parameters affecting the matter power spectrum: dynamical dark energy (w_0, w_a), neutrino mass (m_ν), and the gravitational deviations (γ). Ignoring any of these by fixing a parameter will produce higher figures of merit, at the price of neglecting possibly relevant physics. This seems particularly undesirable in the case of neutrino mass, where we know the physics exists yet we do not know the parameter value.

Figure 8 shows the effect of fixing ω_ν (i.e., $\sum m_\nu$) on the dark energy estimation. The major degeneracy that is artificially broken by *ad hoc* fixing is with the pivot value of the dark energy equation of state, w_p, which decorrelates this value from the time variation w_a. Neglecting neutrino mass or assuming its value makes FOM appear to be 2.3 times higher than it should be. Strong lensing time delays are particularly powerful in the fixed m_ν case, increasing the FOM by 76% rather than the previous 32% of Fig. 5.

If we disallow deviations from general relativity, fixing γ, then the main effect is breaking the degeneracy with σ_8. In such a case galaxy clustering (or weak lensing) is no longer needed to determine σ_8 as the CMB and its lensing do a good job (for example, determining it to 0.01 for CMB + SN, and to 0.007 for CMB + SN + SL). For the combination with galaxy clustering, fixing γ leads to σ_8 constrained a factor 1.7 more tightly than with γ fit. The effect on FOMw is much more modest at just 8%. Fixing both ω_ν and γ basically convolves the effects of each. For the FOM using all probes the total induced tightening is a factor 2.8: i.e., FOMw would be 406 in the commonly used parameter space ignoring m_ν and γ, rather than 147. We emphasize that fixing parameters, apart from restricting physics perhaps unjustifiably, opens the result to bias if the wrong parameter values are used.

V. CONCLUSIONS

The origin of cosmic acceleration is a fundamental mystery of physics, and the subject of active and varied observational efforts. We find and quantify that the newly maturing probe of CMB lensing can play a significant role. Within the next five years maps of the CMB lensing deflection field over wide areas will be obtained, considerably strengthening our cosmological knowledge. These experiments are underway or imminent, and in combination with ongoing or near term dark energy surveys will provide a large step forward in evaluating dark energy, neutrino, gravity, and primordial perturbation properties.

The high-resolution, low-noise, ground-based CMB polarization experiments give powerful leverage. Indeed, in combination with all other survey probes in the commonly used "vanilla plus w_0, w_a" parameter space the result would be a very strong dark energy figure of merit FOM$[w_0, w_a] = 406$. However, it is overly restrictive to assume perfect knowledge of the sum of neutrino masses and the behavior of gravity, both of which affect the growth of structure we are using as a cosmological probe. We present results including simultaneous fits for not only the vanilla parameters but dark energy dynamics w_0 and w_a, gravity γ, and sum of neutrino masses $\sum m_\nu$.

Concentrating on data expected to arrive within the next five years, we examine constraints from realistic near term experiments measuring CMB satellite and ground-based polarization, supernova distances, and the galaxy power spectrum, as the baseline combination of surveys. The complementarity between the different probes is highlighted and quantified. In addition to the cosmological parameter estimation and figures of merit in dark energy and gravity-neutrino planes, we analyze the dependence of the results on the sky area of the CMB space/ground overlap and of galaxy surveys. We further study the impact of weak lensing data.

Interestingly, we find that substantial further leverage can be obtained in supplementing the canonical program with a modest strong lensing time delay survey, requiring of order ~200 orbits on the Hubble Space Telescope, and a tightly systematics-controlled nearby supernova program. This overall combination of experiments would deliver knowledge of the dark energy time variation w_a to 0.25 and of the sum of the neutrino masses to 0.055 eV with data taken by ~2017.

CMB lensing thus acts as a powerful component of a dark energy and cosmology survey program, enabling us to close in on chasing down cosmic acceleration. For further improvements between 2017 and when the next generation of cosmic volume surveys deliver data, promising paths forward include the use of cross-correlations between probes, the development of new probes (just as CMB lensing and strong lensing grew viable), reduction of weak lensing systematics, and the ability to accurately use smaller scales ($k_{\rm max} > 0.125h/{\rm Mpc}$) in the galaxy power spectrum.

ACKNOWLEDGMENTS

This work has been supported in part by the Director, Office of Science, Office of High Energy Physics, of the U.S. Department of Energy under Contract No. DE-AC02-05CH11231 and by World Class University grant No. R32-2009-000-10130-0 through the National Research Foundation, Ministry of Education, Science and Technology of Korea.

[1] E. Komatsu *et al.*, Astrophys. J. Suppl. Ser. **192**, 18 (2011); D. Larson *et al.*, Astrophys. J. Suppl. Ser. **192**, 16 (2011).
[2] C. L. Reichardt *et al.*, Astrophys. J. **694**, 1200 (2009).
[3] M. L. Brown *et al.*, Astrophys. J. **705**, 978 (2009).
[4] H. C. Chiang *et al.*, Astrophys. J. **711**, 1123 (2010).
[5] S. Das *et al.*, Astrophys. J. **729**, 62 (2011); J. Dunkley *et al.*, Astrophys. J. **739**, 52 (2011).
[6] E. Shirokoff *et al.*, Astrophys. J. **736**, 61 (2011); R. Keisler *et al.*, Astrophys. J. **743**, 28 (2011).
[7] P. A. R. Ade *et al.* (Planck Collaboration), Astron. Astrophys. **536**, A1 (2011).
[8] M. D. Niemack *et al.*, Proc. SPIE Int. Soc. Opt. Eng. **7741**, 77411S (2010).
[9] C.-L. Kuo (private communication), http://polar-array.stanford.edu/public/index.html.
[10] A. T. Lee *et al.*, AIP Conf. Proc. **1040**, 66 (2008).
[11] J. J. McMahon *et al.*, AIP Conf. Proc. **1185**, 511 (2009).
[12] S. Das *et al.*, Phys. Rev. Lett. **107**, 021301 (2011).
[13] A. van Engelen *et al.*, Astrophys. J. **756**, 142 (2012).
[14] A. Lewis and A. Challinor, Phys. Rep. **429**, 1 (2006).
[15] B. D. Sherwin *et al.*, Phys. Rev. Lett. **107**, 021302 (2011).
[16] R. de Putter, O. Zahn, and E. V. Linder, Phys. Rev. D **79**, 065033 (2009).
[17] E. V. Linder, Phys. Rev. Lett. **90**, 091301 (2003).
[18] R. de Putter and E. V. Linder, J. Cosmol. Astropart. Phys. 10 (2008) 042.
[19] E. V. Linder, Phys. Rev. D **72**, 043529 (2005).
[20] E. V. Linder and R. N. Cahn, Astropart. Phys. **28**, 481 (2007).
[21] http://snfactory.lbl.gov; G. Aldering *et al.*, Proc. SPIE Int. Soc. Opt. Eng. **4836**, 61 (2002).
[22] http://www.darkenergysurvey.org.
[23] S. Das, R. de Putter, E. V. Linder, and R. Nakajima, arXiv:1102.5090.
[24] http://www.sdss3.org/surveys/boss.php; D. J. Eisenstein *et al.*, Astron. J. **142**, 72 (2011).
[25] E. V. Linder, Phys. Rev. D **84**, 123529 (2011).
[26] R. Fadely, C. R. Keeton, R. Nakajima, and G. M. Bernstein, Astrophys. J. **711**, 246 (2010).
[27] S. H. Suyu, P. J. Marshall, M. W. Auger, S. Hilbert, R. D. Blandford, L. V. E. Koopmans, C. D. Fassnacht, and T. Treu, Astrophys. J. **711**, 201 (2010).
[28] F. Courbin *et al.*, Astron. Astrophys. **536**, A53 (2011).
[29] M. Oguri, Astrophys. J. **660**, 1 (2007).
[30] S. H. Suyu, P. J. Marshall, R. D. Blandford, C. D. Fassnacht, L. V. E. Koopmans, J. P. McKean, and T. Treu, Astrophys. J. **691**, 277 (2009).
[31] S. Suyu (private communication).
[32] S. Suyu, arXiv:1202.0278
[33] http://csp.obs.carnegiescience.edu; S. Kattner *et al.*, Publ. Astron. Soc. Pac. **124**, 114 (2012).